https://ntrs.nasa.gov/search.jsp?R=19850023328 2020-03-20T17:30:30+00:00Z

N85-21[illegible]

RE

Metadata, citation and similar p

by NASA Technical Reports Server

Pittsburgh, PA 15235

ABSTRACT

This paper shows that oxide surface passivation coupled with optimum multilayer anti-reflective coating can provide ~ 3% (absolute) improvement in solar cell efficiency. Use of single-layer AR coating, without passivation, gives cell efficiencies in the range of 15-15.5% on high-quality, 4 ohm-cm as well as 0.1-0.2 ohm-cm float-zone silicon. Oxide surface passivation alone raises the cell efficiency to > 17%. An optimum double-layer AR coating on oxide-passivated cells provides an additional ~ 5-10% improvement over a single-layer AR-coated cell, resulting in cell efficiencies in excess of 18%. Experimentally observed improvements are supported by model calculations and an approach to > 20% efficient cells is discussed.

1. INTRODUCTION

The idealized efficiency[1] of a silicon solar cell is about 25%, assuming the best material and surface parameters achievable to date, although present day cells fall considerably short of this limiting value. This is largely a consequence of heavy doping effects, bandgap narrowing, and high recombination at and near the cell surfaces. The major problems of efficiency improvement fall in the above categories; however, there are additional design requirements for efficient contacts and antireflective coating. Although these areas are well understood, they are not trivial and must be optimized consistent with the device structure. In this paper we will discuss the design, fabrication, and analysis of 18% efficient surface-passivated solar cells on high-quality, 0.1-0.2 ohm-cm float-zone silicon. Results on 4 ohm-cm silicon cells are also shown. Various electrical measurements, along with a simple theoretical model which uses internal recombination velocity to assess minority carrier losses in various regions of the solar cell, are used to analyze the cell data and address the requirements for surface-passivated 20% efficient cells on low-resisitivity silicon.

2. CONSIDERATIONS FOR HIGH-EFFICIENCY SOLAR CELLS

It is clear that high efficiency is a major attribute that will enhance the large-scale applicability of solar photovoltaic systems. Assuming 5% reflector absorption losses, 1% mismatch losses, and 96% packing factor for rectangular cells, 20% efficient cells will be required for 18% efficient

modules. Current module efficiencies are about 12-13% in production. In the last two to three years, solar cell efficiencies have been in the range of 14-17%, even at the research level; however, recent breakthroughs have occurred in single-crystal cell efficiency at the research level. Cell efficiencies in the range of 17-19.1% have been reported by several investigators (Table 1). To achieve 20% or greater efficiency cells, a considerable amount of further research will be required in the areas of:

- Material and carrier lifetime improvements
- Process development
- Design improvements such as surface passivation, reduced heavy doping, and multilayer AR coating
- Tandem cells

Module efficiencies can be further enhanced by:

- Improved packing factor
- Reduced reflection losses from the glass
- Reduced interconnect losses
- Reduced mismatch losses by near-uniform cells

2.1 Material and Carrier Lifetime Considerations

High carrier lifetime is desirable because it improves both J_{sc} and V_{oc}. The best measured lifetime values in silicon to date are on the order of 1 msec, well below the ultimate value based on the radiative band to band recombination. Fossum et al.[11] have hypothesized a vacancy-related fundamental defect in silicon crystals which limits the lifetime in nondegenerate silicon. Based on our experience, it is difficult to detect any deep-level defect in good-quality silicon even with the help of the most sensitive techniques, such as deep-level transient spectroscopy, that are available today. There is some concern about the accuracy of true lifetime or diffusion length measurements, especially when diffusion length becomes greater than the base width.

In Table 1, use of very high-quality low-resistivity (0.1-0.3 ohm-cm) float-zone silicon was a key factor in 17-19.1% efficient cells fabricated by Westinghouse, Spire Corp., and the University of New South Wales. It is not clear why these crystals are much better or less sensitive to process-induced lifetime degradation compared to the majority of low resistivity Czochralski or float-zone crystals. Therefore, there is a need to identify, understand, and minimize the lifetime-limiting centers and develop more reliable techniques for measuring true base diffusion length and surface recombination velocities.

2.2 Process Considerations

High carrier lifetime in the starting silicon becomes academic if processing introduces new defects and unwanted impurities. Special care must be taken during substrate cleaning, and favorable gettering ambients consisting of $POCl_3$ and HCl gas should be utilized whenever possible. Slow

Table 1

Some Recent High-Efficiency Silicon Solar Cells
Tested Under One Sun AM1 Illumination

J_{sc} mA/cm^2	V_{oc} mV	FF	η %	Substrate Resistivity ohm-cm	Source
36.0	625	.805	18.1	0.15	Applied Solar Energy
36.5	610	.775	17.2	10.0	Corporaton
36.2	600	.793	17.2	4.0	Westinghouse
36.0	627	.800	18.1	0.2	Westinghouse
35.9	627	.800	18.1	0.3	Spire Corporation
34.9	643	.813	18.1	0.2	University of New South Wales, Australia
33.0	653	.810	17.5	0.3 Concentrator Cell	Sandia National Laboratories
34.0	624	.820	17.6	0.3 Concentrator Cell	Applied Solar Energy Corporation
35.1	623	.780	17.1	0.3	Catholic University of Leuven, Belgium
36.0	653	.811	19.1	0.1-0.3	University of New South Wales, Australia

cooling and gradual wafer withdrawals from the furnace could also be important in preserving the lifetime of the starting material.

2.3 Design Considerations

If a very high carrier lifetime cannot be obtained in the finished cell, then a clever cell design can still give high-efficiency cells. As suggested by recent model calculations of Sah,[12] 20% efficient p^+-n-n^+ cells can be realized with a base lifetime of 20 μsecs provided that cell thickness is reduced to 50 μm and the back-surface field is 20 μm deep with N_D of 5×10^{18} cm^{-3}. Wolf's[1] design criteria for very high-efficiency cells include equal impurity concentration in the base and emitter up to the onset of heavy doping effects, coupled with reduced surface recombination velocities on the order of 10 cm/sec.

In this paper our own model calculations show that a combination of design features such as surface passivation, reduced heavy doping, and

Table 2

A Comparison of Measured and Calculated Open-Circuit Voltage for High- and Low-Resistivity Solar Cells With and Without Surface Passivation Designs

ID and Cell Design	S_{ejb} cm/sec	S_{eje} cm/sec	J_{ob} pA/cm^2	J_{oe} pA/cm^2	$J_{ob} + J_{oe}$ pA/cm^2	Measured J_{sc} mA/cm^2	Calculated V_{oc} mV	Measured V_{oc} mV	Cell η %
	$N_A = 3.5 \times 10^{15}$, L = 400 μs, W = 250 μm								
No Passivation Cell #2	883	4826	7.9	1.5	9.4	33.4	569	582	15.2
Front and Back Surface Passivation Cell # HIEFY 4-5	517	3340	4.6	1.0	5.6	36.2	584	600	17.2
Passivation and Reduced Heavy Doping	456	117	4.1	0.04	4.14	36.2*	592	-	18.4Δ
	$N_A = 2 \times 10^{17}$, L = 168 μs, W = 375 μm								
No Passivation Cell #C-2	956	12129	0.15	1.3	1.45	31.7	616	612	15.6
Front and Back Surface Passivation Cell #C-8	953	9301	0.15	0.97	1.12	33.2	625	628	17.0
Surface Passivation and Double-Layer AR Cell #C-12	953	9301	0.15	0.97	1.12	36.0	625	627	18.0
Surface Passivation Reduced Heavy Doping, Double-Layer AR	925	332	0.14	0.03	0.17	36.0*	675	-	20.0Δ

*Assumed
ΔExpected

multilayer AR coating can give ~ 20% efficient cells on 0.1-0.3 ohm-cm float-zone silicon with base diffusion lengths in the range of 150 to 200 microns.

3. MODEL CALCULATIONS

We have developed a simplified analytical model to provide guidelines for maximizing V_{oc} and cell efficiency. This model, which is described elsewhere in detail,[2,3] includes the effect of bandgap narrowing, Auger recombination, and recombination at the cell surfaces, but it neglects the electric field effects resulting from the gradient of doping concentrations.[4,5] With the help of this model we can calculate internal recombination velocity (S_e) in any region of the cell using surface recombination velocity (S_o), diffusion length, cell width, and doping density as input parameters. The solar cell is divided into several small elements and S is calculated iteratively from the surfaces toward the junction using the following equation:

$$S_2 = \frac{N_2}{N_1} \frac{D}{L} \exp\left(\Delta V_{G2} - \Delta V_{G1}\right) \frac{S_1 \frac{L}{D} + \tanh\left(\frac{W}{L}\right)}{1 + S_1 \frac{L}{D} \tanh\left(\frac{W}{L}\right)} \qquad (1)$$

where W is the width of the element; (S_1, N_1, ΔV_{G1}) and (S_2, N_2, ΔV_{G2}) are the recombination velocity, doping density, and the bandgap narrowing at the two boundaries of the element; and D and L are the diffusivity and diffusion length of the minority carriers within the element. The model uses empirical equations to calculate diffusivity, diffusion length, and bandgap narrowing primarily from the doping density.[2,3]

Examples of internal recombination velocity plots are shown in Figures 1 and 2. Figure 1 shows the calculations for 4 ohm-cm cells with a base diffusion length of 400 μm, and Figure 2 is for 0.1-0.2 ohm-cm cells with a base diffusion length of 168 μm. Each figure includes the calculation for three different back-surface field (BSF) and emitter designs, namely: a) no surface passivation, b) surface passivation where S_o is reduced to 500 cm/sec, and c) surface passivation plus reduced heavy doping where the surface dopant concentration has been lowered from 2×10^{20} cm^{-3} to 10^{19} cm^{-3}. S_o at the metal and bare silicon surface is assumed to be 10^6 cm/sec and 10^4 cm/sec, respectively. A junction depth of 0.3 μm and a BSF width of 0.5 μm were determined by spreading resistance measurements on the actual cells. Exponential doping profiles are assumed in the diffused regions, and the doping density at the emitter depletion boundary in Figures 1 and 2 has been estimated to be 1×10^{17} cm^{-3} and 3×10^{17} cm^{-3}, respectively.

Using the values of the internal recombination velocities at the depletion region boundaries in Figures 1 and 2, total reverse saturation current (J_o) for any case can be calculated according to:

$$J_o = J_{ob} + J_{oe} = q\, n_i^2 \left(\frac{S_{ejb}}{N_A} + \frac{S_{eje}}{N_D}\right) \qquad (2)$$

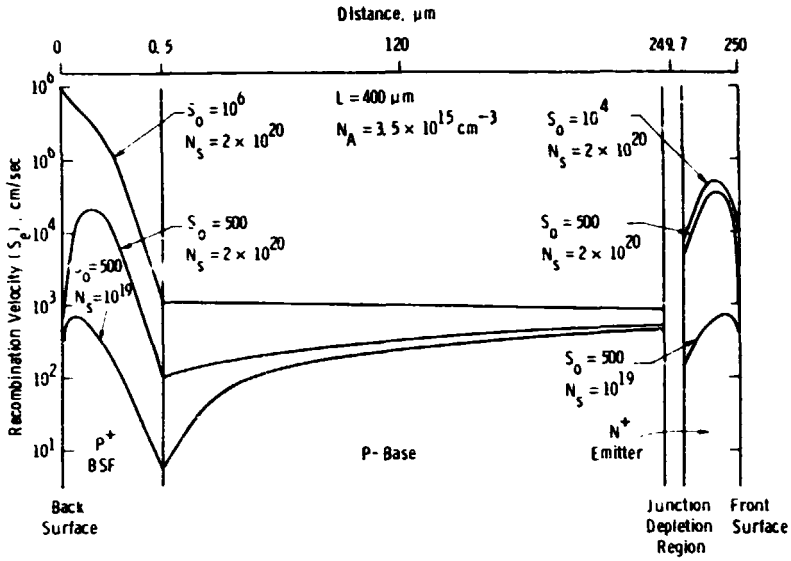

Figure 1. Model calculations and internal recombination velocity plots for 4 ohm-cm base cells with a base diffusion length of 400 microns.

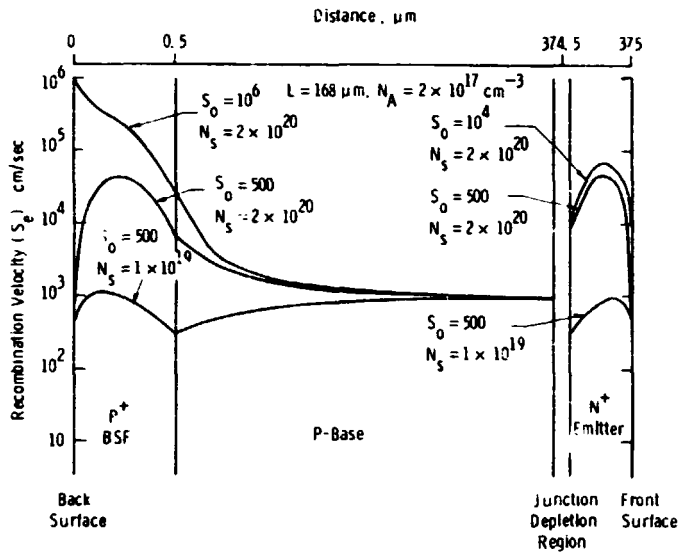

Figure 2. Model calculations and internal recombination velocity plots for 0.1-0.2 ohm-cm base cells with a base diffusion length of 168 microns.

where J_{ob} and J_{oe} represent the base and emitter contribution of J_o and (S_{ejb}, N_A) and (S_{eje}, N_D) are the recombination velocity and the doping density at the depletion region boundary in the base and emitter, respectively. Finally, V_{oc} is calculated from

$$V_{oc} = \frac{KT}{q} \ln \left(\frac{J_{sc}}{J_o}\right)$$

where J_{sc} is either estimated or measured short-circuit current density. Table 2 shows the calculated J_o and V_{oc} for various cell designs in Figures 1 and 2.

4. EXPERIMENTAL WORK

Following the guidelines of our model calculations, we fabricated oxide-passivated cells on high-quality a) 0.1-0.2 ohm-cm, boron-doped, (100), 15 mils thick float-zone silicon and b) 4 ohm-cm, boron-doped, (111) float-zone and dendritic web silicon. The baseline cell structure was n^+-p-p^+, where the n^+ emitter was formed by a 850°C $POCl_3$ diffusion which resulted in a junction depth of 0.3 μm and a sheet resistance of 60-80 ohm/square. The p^+ back-surface field was fabricated by a 950°C boron diffusion. Thermal oxide for passivation was grown at 800°C, which resulted in an oxide thickness of ~ 100 Å on top of the n^+ region and ~ 50 Å on the p^+ surface. About 600 Å thick single-layer AR coating was applied by a spin-on process on the passivated cells. AR coating thickness on the unpassivated cells was ~ 750 Å. In selected instances a double-layer AR coating was applied on the oxide-passivated cells by a spin-on process. The double-layer AR coating consists of 475 Å TiO_2 and 980 Å SiO_2 layers on top of 100 Å passivating oxide. Ti-Pd-Ag contacts were made on front and back, and the front grid design had an area coverage of 2%.

Both reflectivity and spectral response measurements were performed over a wavelength range of 0.4 to 1.1 μm to obtain the internal quantum efficiency. In selected instances, minority carrier lifetime in the cells was measured by the open-circuit voltage decay (OCVD) technique, where the injection current was made equal to the short-circuit current.

5. RESULTS

Table 3 shows the data for the 4 ohm-cm float-zone silicon cells, with and without oxide surface passivation. Without passivation, J_{sc} is ~ 33 mA/cm^2, V_{oc} is ~580 mV, and cell efficiency is ~ 15%. With both surfaces passviated, the cell efficiencies are in excess of 17%, with V_{oc} ~ 600 mV and J_{sc} ~ 36 mA/cm^2. Dark I-V measurements showed that oxide passivation reduces J_o by about a factor of two.[3] Quantum efficiency plots in Figure 3 clearly show that front- and back-surface passivation enhances the short- and long-wavelength responses of the cell. OCVD lifetime in the 17.2% cells was 50 μsecs, corresponding to a diffusion length of ~ 400 μm, which was used in the model calculations in Figure 1.

Table 4 shows the data for the passivated and unpassivated 0.1-0.2 ohm-cm base cells. Unpassivated cell efficiencies are ~ 15.5%, with J_{sc} of 31.5 mA/cm^2 and V_{oc} of 612 mV. After oxide passivation, cell efficiencies approach 17% with J_{sc} = 33 mA/cm^2 and V_{oc} = 627 mV. Dark I-V data showed a decrease in J_o from 7.1 x 10^{-13} A/cm^2 to 5.0 x 10^{-13} A/cm^2. Quantum efficiency plots in Figure 4 show that oxide passivation on this low-resistivity silicon increases only the short-wavelength response, but has negligible effect on the long-wavelength response. OCVD lifetime on these

Table 3

Solar Cell Data on 4 ohm-cm Float-Zone Silicon With and Without Oxide Passivation With Single-Layer AR Coating

Cell ID	J_{sc} mA/cm^2	V_{oc} Volts	Fill Factor	Efficiency %
		WITHOUT PASSIVATION		
1	33.3	0.582	0.767	14.8
2	33.4	0.582	0.780	15.2
		WITH PASSIVATION		
HIEFY 4-4	36.1	0.599	0.794	17.1
-5	36.2	0.600	0.793	17.2

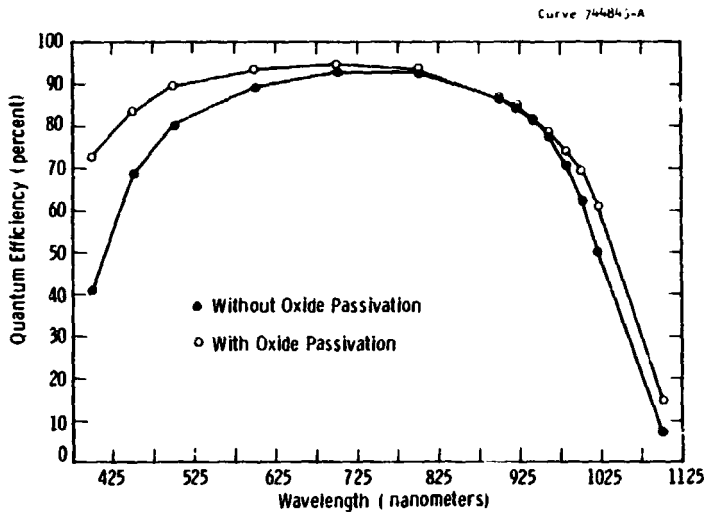

Figure 3. Internal quantum efficiency plots for a 15.2% unpassivated cell and a 17.2% efficient oxide-passivated cell on 4 ohm-cm float-zone silicon.

cells was ~ 168 μm, which was used in the model calculations in Figure 2. Table 4 also shows that double-layer AR coating increased J_{sc} from 33 mA/cm^2 to ~ 36 mA/cm^2 and gave ≥ 18% efficient cells. Figure 5 shows the measured spectral reflectivities on single-layer AR-coated 17% efficient cells and double-layer AR-coated 18% efficient cells.

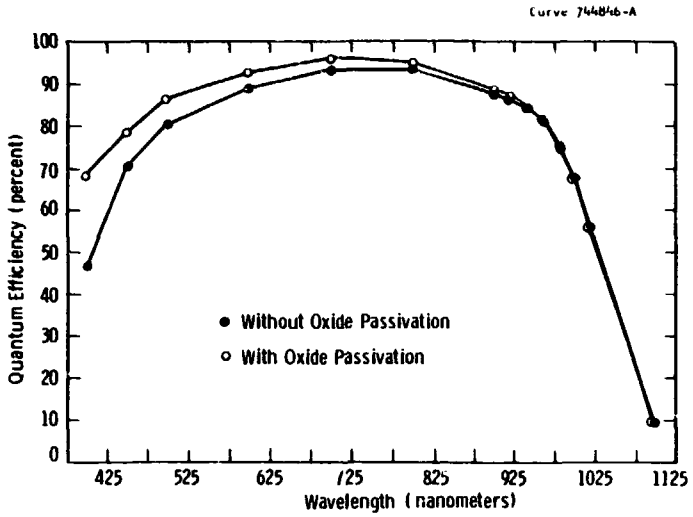

ORIGINAL PAGE IS
OF POOR QUALITY

Figure 4. Internal quantum efficiency plots for a 15.6% efficient unpassivated cell and a 16.9% efficient oxide-passivated cell on 0.1-0.2 ohm-cm float-zone silicon.

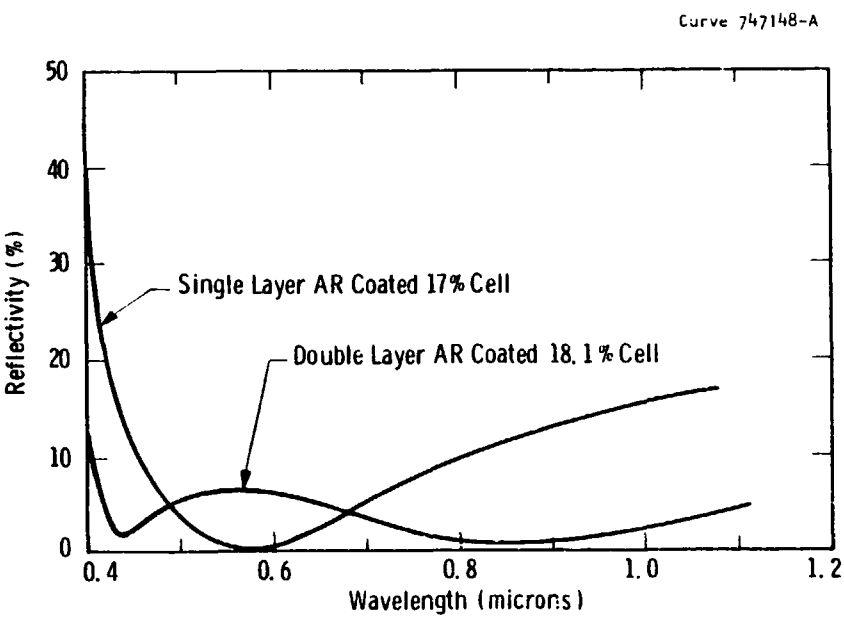

Figure 5. Measured reflectivities of single-layer AR-coated 17% efficient cell and double-layer AR-coated cell.

Oxide-passivated cells were also fabricated on 4 ohm-cm dendritic web silicon crystals. Table 5 shows that without oxide passivation, good-quality web crystals give average efficiency of ~ 14.5%, but with oxide passivation the cell efficiencies are ~ 16%. As in the case of 4 ohm-cm float-zone silicon cells, an oxide passivation-induced 1 to 2% increase in web cell efficiency was associated with an increase in J_{sc} and V_{oc} and a reduction in J_o.

Table 4

Solar Cell Data on 0.1-0.2 ohm-cm Float-Zone Silicon With and Without Oxide Passivation

Cell ID	J_{sc} mA/cm^2	V_{oc} Volts	Fill Factor	Efficiency %
		WITHOUT OXIDE PASSIVATION		
C-2	31.8	0.613	0.802	15.6
C-5	31.7	0.612	0.797	15.5
		WITH OXIDE PASSIVATION		
C-7	33.0	0.627	0.815	16.9
C-8	33.2	0.628	0.815	17.0
		PASSIVATION AND DOUBLE-LAYER AR		
C-9	34.7	0.626	0.810	17.6
C-10	35.1	0.624	0.803	17.6
C-11	36.0	0.620	0.808	18.0
C-12	36.0	0.627	0.800	18.1

Table 5

Solar Cell Data on 4 ohm-cm Dendritic Web Silicon With and Without Oxide Passivation

Cell ID	J_{sc} mA/cm^2	V_{oc} Volts	Fill Factor	Efficiency %
		WITHOUT PASSIVATION		
W6	32.7	0.575	0.782	14.7
W7	33.1	0.577	0.784	15.0
		WITH OXIDE PASSIVATION		
W1	34.6	0.584	0.784	15.9
W2	34.5	0.586	0.794	15.8

6. DISCUSSION

Table 2 shows that oxide passivation coupled with careful cell processing can produce cell efficiencies greater than 17% (AM1) on high-quality 4 ohm-cm float-zone silicon, with $V_{oc} \sim 600$ mV and $J_{sc} \sim 36$ mA/cm^2. This corresponds to a ~ 18 mV increase in V_{oc}, 3 mA/cm^2 increase in J_{sc}, and 2% improvement in absolute cell efficiency compared to the unpassivated cells. Model calculations in Figure 1 and Table 2 for the 4 ohm-cm base cells indicate that without any surface passivation, J_{ob} and J_{oe} contribute appre-

ciably to the total J_o; therefore, both front- and back-surface passivation become important in reducing J_o or improving V_{oc}. For example, Table 2 shows that: a) without any passivation, J_o = 9.4 pA/cm^2 and the calculated V_{oc} is 569 mV; b) with front-surface passivation alone, J_o = 7.9 + 1.0 = 8.9 pA; c) with only back-surface passivation, J_o = 4.6 + 1.5 = 6.1 pA; and d) with both surfaces passivated, J_o = 5.6 pA, resulting in a calculated V_{oc} of 584 mV. Thus, model calculations predict an increase of 15 mV in V_{oc} if both surfaces of a 4 ohm-cm cell are passivated and its base diffusion length is 400 μm. This is in very good agreement with the experimentally observed increase of 18 mV in V_{oc}. However, it should be noted in Table 2 that the absolute values of calculated V_{oc} are about 15 mV smaller than the measured values. This difference can be attributed to a number of assumptions and estimated inputs that went into the model calculations, e.g., surface recombination velocities, exponential doping profiles, diffusion length obtained by OCVD lifetime, and estimated doping density at the depletion region boundary in the emitter. More accurate values of the above parameters are needed for precise modeling; nevertheless, such model calculations provide very useful guidelines as to what should be done to which region of the solar cell in order to obtain high V_{oc}.

Figure 2 and Table 2 show a similar calculation for a 375 μm thick cell on 0.1-0.2 ohm-cm silicon with a base diffusion length of 168 μm. Unlike the 4 ohm-cm cells, here J_{oe} dominates J_o,[9] with or without surface passivation. In addition, J_{ob} remained unchanged (0.15 pA/cm^2) after back-surface passivation, because the minority carrier diffusion length in the base is much smaller than the thickness of the base. Therefore, back-surface passivation in these low-resistivity cells becomes unimportant, and only the front-surface passivation contributes to the increase in V_{oc}. A calculated increase of 9 mV in V_{oc} is in good agreement with the observed increase of 13 mV, considering the number of model assumptions. Notice in Table 2 that the calculated values of V_{oc} are in much better agreement (± 4 mV) with the measured values for the low-resistivity cells. This is probably the result of the better estimates for the model inputs for this case.

In the 4 ohm-cm base cells, we measured a 3 mA/cm^2 improvement in J_{sc} compared to 1.5 mA/cm^2 in the low-resistivity cells as a result of oxide passivation. This can also be explained in terms of the difference in the effectiveness of back-surface passivation in the two cells. In the low-resistivity cells, diffusion length to cell thickness ratio (L/W) is much less than one; therefore, reduced recombination at the back surface does not improve the collection or quantum efficiency of the carriers generated by the long-wavelength photons near the back surface (Figure 4). The improved J_{sc} in the low-resistivity cells only results from front-surface passivation, which enhances the quantum efficiency of the short wavelengths (Figure 4). In the 4 ohm-cm base cells, (L/W) is much greater than one; therefore, we observe an improvement in short- as well as long-wavelength response (Figure 3).

Table 4 shows that the use of double-layer AR coating raises the low-resistivity cell efficiencies from 17% to 18.1%. Single-layer AR-coated 17% efficient cells and double-layer AR-coated 18.1% cells on 0.1-0.2 ohm-cm float-zone silicon were analyzed in detail by spectral response and reflectivity measurements. Figure 5 shows a comparison of the measured reflectivity of the two cells as a function of wavelength. The double-layer AR-coated cell has smaller integral reflectivity compared to the single-layer

AR-coated cell. However, as shown in Figure 6, their internal quantum efficiency as a function of wavelength is virtually similar. It is important to remember that in the calculation of internal quantum efficiency, the effects of reflectivity are removed; therefore, identical internal quantum efficiencies imply that the interior quality of the two cells is nearly the same. Thus, the difference in the cell efficiency is primarily due to the difference in the reflectivity of the AR coatings. This is consistent with the cell data in Table 4, which show that the ~ 2 to 3 mA/cm^2 increase in short-circuit current is the main reason for increased cell efficiency from 17 to 18.1%.

Table 2 also shows model calculations for a cell design with reduced heavy doping in the emitter and the BSF regions. In this case dopant concentration at the surfaces has been reduced from 2×10^{20} cm^{-3} to 10^{19} cm^{-3}. It is interesting to note that reduced heavy doping in a 4 ohm-cm base cell gives additional improvement of only 8 mV (592-584) in V_{oc}, but in the low-resistivity case the calculated improvement is 48 mV (673-625), neglecting the drift field effects. This is because reduced heavy doping in the BSF region does not change J_{ob} very much, but reduced doping in the emitter lowers J_{oe} by more than an order of magnitude (Table 2). Since the V_{oc} of the oxide-passivated 4 ohm-cm cells is controlled by J_{ob}, reduced heavy

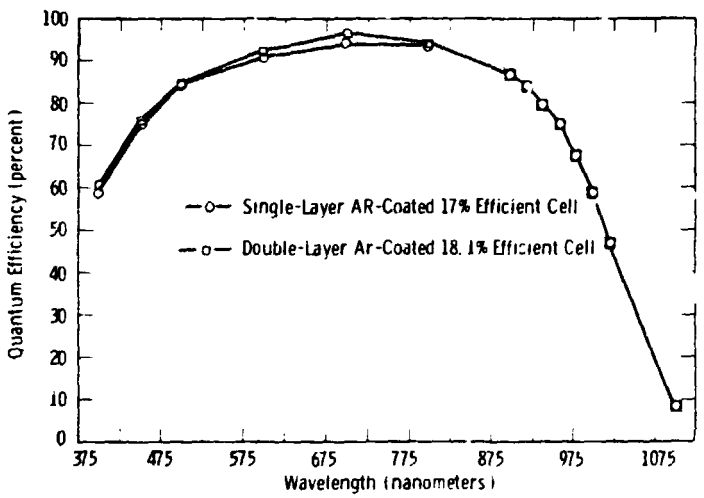

Figure 6. Internal quantum efficiency versus wavelength plots for a 17% efficient single-layer AR-coated cell and an 18.1% efficient double-layer AR-coated cell.

doping has little effect on V_{oc}. The V_{oc} of oxide-passivated 0.1-0.2 ohm-cm cells is controlled by J_{oe}; therefore, reduced heavy doping in the emitter increases V_{oc} very significantly. Therefore, use of multilayer AR coating and reduced heavy doping can make these low-resistivity surface-passivated cells (Table 4) 20% efficient with V_{oc} of 675 mV, J_{sc} of 36 mA/cm^2, and fill factor of 0.82. Calculations in Table 2 point out that at 20% efficiency, V_{oc} of these low-resistivity cells will become base-limited ($J_{ob} >> J_{oe}$). Therefore, in order to obtain greater than 20% efficient cells, either base thickness will have to be reduced or higher base diffusion lengths will be required. Some experiments are being conducted to verify this model design.

CONCLUSIONS

Consistent with our model calculations, we were able to improve open-circuit voltage and short-circuit current by oxide passivation of the cell surfaces. Oxide-passivated cell efficiencies on 4 ohm-cm as well as 0.1-0.2 ohm-cm float-zone silicon were 17% compared to 15 to 15.5% without surface passivation. Use of double-layer AR coating raised the low-resistivity cell efficiencies from 17% to 18.1%. In 4 ohm-cm cells, both front- and back-surface passivation was important, and their combined influence increased V_{oc} by 18 mV and J_{sc} by 3 mA/cm^2. In 0.1-0.2 ohm-cm cells, where diffusion length was much smaller than the cell thickness, back-surface passivation did not help significantly. In these cells, V_{oc} went up by 13 mV and J_{sc} increased by 1.5 mA/cm^2. Our model calculations indicate that in low-resistivity cells, J_{oe} dominates J_o; therefore, back-surface passivation does not improve V_{oc}. However, front-surface passivation reduces J_o and improves the short-wavelength response quite significantly. Model calculations indicate that oxide passivation coupled with reduced heavy doping in the emitter can give a very substantial increase in V_{oc} in the low-resistivity cells with efficiencies of 20%.

REFERENCES

1. M. Wolf, Proc. of 14th IEEE Photovoltaic Specialists Conf., p. 674 (1980).

2. J. R. Davis and A. Rohatgi, Proc. of 14th IEEE Photovoltaic Specialists Conf., p. 569 (1980).

3. A Rohatgi and P. Rai-Choudhury, IEEE Trans. on Electron Devices, ED-31, No. 5, p. 596 (1984).

4. M. Wolf, Proc. of 14th IEEE Photovoltaic Specialists Conf., p. 563 (1980).

5. M. P. Godlewski, C. R. Barona, and H. W. Brandhorst, Proc. 10th IEEE Photovoltaic Specialists Conf., p. 40 (1973).

6. A. Rohatgi, J. R. Davis, R. H. Hopkins, P. Rai-Choudhury, P. G. McMullin nad J. R. McCormick, J. Solid State Electronics, Vol. 22, p. 415 (1980).

7. A. Neugroschel, F. Lindholm and C. T. Sah, IEEE Trans. on Electron Device, Vol. ED-24, p. 662 (1974).

8. H. J. Hovel, "Semiconductor and Semimetals," Solar Cells, Vol. II, Academic Press (1975).

9. J. G. Fossum, F. A. Lindholm and M. S. Shibib, IEEE Trans. on Electron Devices, Vol. ED-26, p. 1294 (1979).

10. A. Rohatgi et al., Second Monthly Report on "Research on the Basic Understanding of High Efficiency in Silicon Solar Cells," SERI Contract No. XB-3-02000-4.

11. J. G. Fossum and D. S. Lee, Solid State Electronics, Vol. 25 (8), p. 741 (1982).

12. C. T. Sah, "Study of Relationships of Material Properties and High-Efficiency Solar Cell Performance on Material Composition," First Technical Report, DOE/JPL Contract No. 956289-83/1, July 1983.

ACKNOWLEDGEMENTS

The authors would like to acknowledge the invaluable contribution of the late J. R. Davis for device modelling and guidance. They would also like to thank T. W. O'Keeffe, D. L. Meier, and D. N. Schmidt for special response measurements; T. W. O'Keeffe, B. Yoldas, and N. J. Rooney for double-layer AR coating; J. B. McNally, F. S. Youngk, and G. Machiko for cell processing; S. Karakoro help in cell testing, computer programming, and model calculations; and G. S. Law for reading and preparing the manuscript. This work was supported by SERI Contract No. XB-3-02090-4 and by the U.S. Department of Energy under prime Contract No. DE-AC02-83CH10093.

CISZEK: Ajeet, could you comment whether there is any influence on the process or the temperature of the oxidation that you use to create your passivation -- on the effectiveness of it?

ROHATGI: Yes, that's a very good question. That passivating oxide is not so easy to grow, because first of all you are growing it on a highly doped surface. It is not like growing an oxide on a silicon wedge, as you do in MOS. So the quality is very critical and the thickness control becomes difficult, especially when you are making such types of cells, because the oxidation rates on n^+ and p^+ are very different. On n^+ the oxidation rate is about three times faster than on the p^+. So it is very critical that you process your device under well-controlled conditions for the oxidation step. You almost have to tailor the oxidation in-house, because it is very sensitive to the processing condition. The thickness there is very critical. If you are off by 30 to 40 seconds you find out that you have exceeded the oxide thickness that is optimum for the passivation and the advantage that you are going to get from anti-reflection coating. But if it is very thick you are going to get hurt in reflection losses.

MILSTEIN: Basically, what I want to do is to confirm some of the hydrogen passivation work that Steve and Ajeet have talked about. We also have passivated a string of cells. These were provided by Bob Campbell; they are made on web. I presented most of this at the IEEE meeting, but we have some further data. The point that Ajeet made on improving efficiency, I think is very important. All of this is published, and will be out in the IEEE Proceedings. But basically, if you look at some of the not-even-so-good cells, you see a 1.5 efficiency. The numbers are hard to read. You will see full one point efficiency improvements on some of the others, again, on cells that were not all AR-coated. We have also looked at the spectral-response data. When Ajeet mentioned his results we took a look at some of ours, and I'll show you two unpassivated cells that we did. Here is cell 10, which was passivated, and here is cell 3, which was not passivated, and if I can line them up we find that for one of the cells the response, in fact, improved; for the other, it did not change very much from virgin cells that had not been passivated in any way. The upper curve is cell 5 and the lower curve is again cell 10, passivated, and you can see that there has been virtually no change there. So the hydrogen passivation clearly is doing things and it is not a one-shot result, it's been seen by more groups than one. The question is, what's going on, and are we going to work on that problem? I might point out that we have an experiment in progress too. We took two pieces of web, one as-received, and after about a 30-minute implant, pumping as much hydrogen as we could, we sent it off to NBS to have them look at it with neutron activation to try to locate hydrogen in the sample.

QUESTION: Just to follow up on what you said, we also have attempted to find out where the hydrogen is located by neutron resonance reaction technique, where we come with nitrogen 15, which reacts very strongly with hydrogen gas. This measurement was done at the University of Western Ontario, by

Professor Tong, and what we found was that 5 ppm hydrogen is present right at the surface, and this concentration goes down to about 1 ppm when you are 1,000 Å deep. Unfortunately, the detection limit is only 1 ppm, so we were not sure whether we had hydrogen beyond 1,000 Å, which is well within the emitter depth that we have. So we have been able to detect hydrogen at least as deep as 1,000 Å, and it could be beyond that.

RAO: Ajeet, in all of your data on that material with the hydrogen passivation and all the other data that other people have presented, I think you have one piece of data where you show the efficiency before AR coating and then after AR coating. I think, if I'm not wrong, the rest of the data including the one Joe presented just now don't show what happens after the AR coating. Looking at your data, the AR coating only improves by about 36% in your hydrogen-passivated cell, which is much lower than the 43% that you are talking about.

ROHATGI: There is a very good reason for that, because this AR coating was applied after the cell was finished, and when you try to spin the AR coating with the grid lines you never get the kind of improvement that you get when you put on the AR coating without the grids -- because when you are spinning it, you don't get the same thickness of AR coating near the grid lines.

RAO: So you anticipate that you will be able to get the 40% to 43% improvement with AR coating on the hydrogenated cells?

ROHATGI: No, this experiment was not done for that. I think we will have to modify our process sequence a little bit. We will have to do hydrogen-ion implantation at a different stage; we will not do it at this stage. It may be even more interesting to find out that hydrogen-ion implantation really works from the back, and this is another reason for looking into that. That way we don't have to do anything to the front. You finish the whole cell and before you put on the back metal you hit the cell with hydrogen-ion implantation and then put on the back metal. So you have to play some clever games with cell processing when you get to this stage.

TURNER: Your optical optimization calculation implied that you were using an oxide layer that was only 100 Å thick. Was that really what you used?

ROHATGI: For the oxide passivation, that's the lowest layer, which is the passivating oxide. Then on top of that we put 475 Å of TiO_2 and then on top of that we have 986 Å of SiO_2.

TURNER: But you got good passivation out of 100 Å of oxide, and that's very good.

ROHATGI: You don't want to go thicker than that -- otherwise it's going to hurt you in the reflection losses.

SARIOTIS: I don't know if I missed it or not: did you mention the area of these cells you discussed?

ROHATGI: Most of the cells are 1 x 1 cm; we are now making cells that are 4 cm square.

SAKIOTIS: Do you have any results on the larger ones?

ROHATGI: Yes, larger ones are not quite as good. The 18.1% cell that you saw is 1 x 1 but the larger one is about 17.8. So we have some difficulty. But they are not more than 4 cm square in any case.

LESK: The nuclear people at Westinghouse have reported that above a few times of 10^{19} hydrogen, there is loss of hydrogen at the surface, and you are doping at 10^{18} I'm wondering if anybody has looked at the possibility that hydrogen implant at these levels may be removing something from the surface area that may have been hurting us in improving the characteristics.

ROHATGI: Okay, if we did the reflectivity measurement to see if we have modified the surface in any sense and -- in at least reflective measurement within what we have -- done anything drastic to the surface, the reflectivity we did before and after the implantation was identical. But we are not sure if we are removing anything, and that's a very good point. We should really do the spreading with this measurement to see if we have actually taken something off and our surface dopant concentration has changed.

QUESTION: May I make just a short comment? I have worked with hydrogen implantation years ago using high energy and pumped in at 10^{18}. It is my experience if you go that high that hydrogen forms bubbles in silicon, so if you go to lower energy then it's most likely that you remove some from the surface.

ROHATGI: That's a good comment. I don't think we know the answer to what we have inside our cell at this point. We don't know where the hydrogen is located or if it has formed any bubbles. We are just trying to do more measurements to find out more about it.

YOO: What is your oxide passivation temperature and time, roughly?

ROHATGI: It's a low-temperature oxide, it's about 800°C, and the time you have to set depending on what kind of dopant surface concentration you have, because oxidation rate, as I mentioned, is a function of how heavy doping you have. So there is no real fixed time. If you are working with low surface doping concentration, you have to go to longer times.